Fragmentation Mechanisms of Product Ions from Protonated Tripeptides†

Houssain El Aribi,§ Galina Orlova,# Christopher F. Rodriquez,‡ David R. P. Almeida, Alan C. Hopkinson, and K. W. Michael Siu*

Department of Chemistry and Centre for Research in Mass Spectrometry, York University, 4700 Keele Street, Toronto, Ontario, Canada M3J 1P3

Received: August 6, 2004; In Final Form: September 15, 2004

Dissociation chemistries of the primary fragment ions from the tripeptides, GAG and AGG, were examined both experimentally and theoretically, and compared with those from GGG [El Aribi, H.; Rodriquez, C. F.; Almeida, D. R. P.; Ling, Y.; Mak, W. W.-N.; Hopkinson, A. C.; Siu, K. W. M. *J. Am. Chem. Soc.* **2003**, *125*, 9229−9236]. Findings in this study with GAG and AGG confirm and extend those in the earlier study on GGG. Fragmentation of the b_2 to a_2 ion from GAG and AGG is qualitatively similar to that from GGG; stabilization by the methyl group, however, results in generally lower energies for GAG. Fragmentation of the a_2 ion from GAG produces both the a_1 (protonated methanimine) and the internal iminium ion (protonated ethanimine). By contrast, fragmentation of the a_2 ion from AGG produces only the a_1 ion (protonated ethanimine). In GAG, formation of the internal iminium ion requires an intramolecular proton transfer in the proton-bridged complex after cleavage of CO, which is absent in AGG. The a_1 ion from GAG is postulated to form via cleavage of the vibrationally excited proton-bridged complex prior to proton transfer, favored under higher collision-energy conditions. The critical transition state in the fragmentation of the b_2 to a_1 ion is best described as a complex between the a_1 ion and a carbene. Although details differ, in both GAG and AGG, there is a proton transfer from the terminal amino group to the carbene carbon and a second proton transfer from the ring nitrogen back to the terminal amino group. Separation of the components then yields the a_1 ion and a neutral oxazolone.

Introduction

Fragmentation of protonated peptides constitutes the basis for gas-phase microsequencing in proteomics, a field in which the enabling technology is tandem mass spectrometry.[1] Under collision-induced dissociation (CID) conditions, protonated peptides fragment along the peptide backbone to produce primarily b, y, and a ions. A low-energy (<100 eV) product

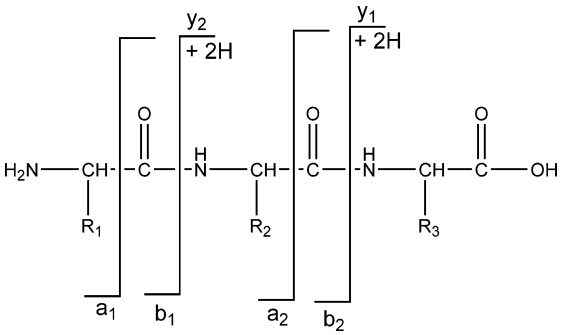

ion spectrum typically consists of a series of fragment ions that reflect the amino acid sequence. The fragmentation chemistry is rich as the 20 amino acid residues exert varying degrees of influence on the dissociation. Typically a CID spectrum comprises many product ions from which the residues' sequence can be constructed.[2−11]

Efforts in proteomics require rapid analysis of a large number of CID spectra, which can realistically only be handled via an informatic approach. A major limitation to universal and reliable automated sequencing is that existing sequencing algorithms[12−14] are limited in that the spectra are interpreted against a list of all possible fragments, without taking into consideration the relative propensities for fragmentation. To consider fragmentation probabilities requires a thorough understanding of dissociation mechanisms, which are at present not well-understood even for peptides comprising "simple" residues. In the past decade, a consensus has developed regarding the principal driving force in peptide fragmentation: the dissociation is charge induced and occurs proximal to the "ionizing" proton.[15−23] Collisional activation mobilizes the proton along the peptide backbone and leads to diverse fragmentation products. In recent years, this proton mobilization and the (direct and indirect) products that it induces have been the subject of a number of investigations.[24−40] A number of these studies used first-principle methods (ab initio and density functional theory (DFT)) to model the fragmentation chemistry.[30−40] One of these[39] employed threshold collision-induced dissociation data to gauge fragmentation mechanisms of protonated triglycine and its primary dissociation products, and reported a number of novel findings.

In particular, it was reported that the lowest energy conformer of the a_2 ion is not an iminium ion, as commonly believed,[2,24−26,32,41] but is a protonated 4-imidazolidone that has a cyclic five-membered-ring structure. In addition, fragmentation of the b_2 ion, a protonated oxazolone,[24,25,36] to the a_1 ion does

* Address correspondence to this author. Phone: (416)650-8021. Fax: (416)736-5936. E-mail: kwmsiu@yorku.ca.

† Material taken from the Ph.D. dissertation of H.E.A., York University, December, 2003; presented at the 50th ASMS Conference, Orlando, FL, June 2−6, 2002.

§ Current address: MDS Sciex, 71 Four Valley Drive, Concord, Ontario, Canada L4K 4V8.

Current address: Department of Chemistry, St. Francis Xavier University, Antigonish, Nova Scotia, Canada B2G 2W5.

‡ Current address: Department of Chemistry, McNeese State University, 221D Kirkman Hall, 4205 Ryan Street, Lake Charles, LA 70609.

10.1021/jp046449m CCC: $27.50
Published on Web 11/06/2004

TABLE 1: Relative Enthalpies at 0 K ($\Delta H°_0$) and Relative Free Energies at 298 K ($\Delta G°_{298}$) for GAG, AGG, and GGG[a] (kcal/mol)

	$\Delta H°_0$			$\Delta G°_{298}$		
structure[b]	GAG	AGG	GGG	GAG	AGG	GGG
1	0.0	0.0	0.0	0.0	0.0	0.0
2	12.2	22.4	22.1	6.9	18.3	17.9
3 + CO	13.8	24.7	24.5	2.3	13.6	13.1
4 + CO	11.6	10.8	14.2	1.6	0.9	4.2
5 + 2CO	27.7	20.1	30.2	−0.8	−2.9	7.7
6	NA[c]	28.0	NA	NA	23.9	NA
7	NA	18.1	NA	NA	15.6	NA
8	20.6	14.6	20.7	16.9	11.2	18.1
9	12.8	NA	11.8	10.9	NA	10.0
10	13.5	1.2	11.8	11.6	−1.2	9.9
11 + a_1	34.2	17.2	31.3	22.8	5.2	20.3
TS(1→2)	29.9	33.7	32.9	28.3	31.3	30.7
TS(3→4) + CO	26.0	35.7	35.9	14.9	24.9	25.0
TS(3→5) + CO	45.6	45.7	49.9	31.4	32.2	36.5
TS(1→6)	NA	31.4	NA	NA	26.3	NA
TS(7→8)	NA	16.6	NA	NA	13.1	NA
TS(1→8)	43.2	NA	41.5	41.0	NA	39.3
TS(8→9)	21.4	NA	21.5	19.7	NA	19.9
TS(9→10)	11.9	NA	10.6	10.4	NA	9.0
TS(8→10)	NA	16.2	NA	NA	14.2	NA

[a] Taken from ref 39. [b] Primes have been dropped in this comparison. [c] NA = not applicable.

not proceed via a mechanism that results in HNCO and $H_2C{=}C{=}O$ as byproducts,[26,28] but proceeds via a transition state that contains an incipient a_1 ion and an incipient carbene. Lastly, fragmentation of the a_2 to the a_1 ion proceeds via a transition state structure that comprises the a_1 ion, CO, and an imine as incipient components.

Here we report additional and confirmatory evidence for the above findings using the primary product ions of protonated glycylalanylglycine (GAG) and alanylglycylglycine (AGG). The methyl group in the alanyl residue stabilizes a proximal charge and permits differentiation between the first and the second residue. The fragmentation reactions of these two tripeptides and the energetics of their products will be compared with those of triglycine.

Computational Method

Calculations were performed with Gaussian 98.[42] Density functional theory (DFT) with the hydrid B3LYP exchange-correlation functional,[43−45] in conjunction with the 6-31++G-(d,p) basis set,[46−51] was employed for structure optimizations and for the characterization of critical points using harmonic vibrational frequency calculations. Intrinsic reaction coordinate calculations[52,53] were carried out to establish the minima associated with particular transition states. Previous investigations have established that DFT calculations at the B3LYP/6-31++G(d,p) level of theory perform satisfactorily for molecules, such as protonated peptides, in which hydrogen bonding is an important structural feature.[36−40,54,55] DFT calculations employing hybrid exchange-correlation functionals such as B3LYP correctly and accurately describe this relatively weak, but important, bond that is responsible for many structural details of protonated peptides and their fragmentation products. The Supporting Information lists the energies of the ions and neutrals relevant to the dissociation of GAG and AGG (Table 1S). GAG-derived ions are numbered in regular numerals. AGG-derived ones are numbered in primed numerals; structures with identical numerals are analogous. Cartesian coordinates of the structures derived from GAG and AGG are also shown in the Supporting Information, Tables 2S and 3S, respectively. Table 1 shows a comparison of the calculated relative enthalpies at 0 K ($\Delta H°_0$) and relative free energies at 298 K ($\Delta G°_{298}$) for the dissociations of GAG and AGG with that of GGG in ref 39. This earlier work[39] labeled the GGG fragment ions differently; the energetics for GGG-derived ions shown in Table 1 are those ions that are analogous to the ones formed from GAG and AGG.

Experimental Method

The experimental details were similar to those used in previous studies.[39,56,57] Threshold CID measurements were conducted on a PE SCIEX API III triple-quadrupole mass spectrometer (Concord, Ontario). The tripeptides, GAG and AGG, were commercially available from Sigma (St. Louis, MO); all chemicals were from Sigma and Aldrich (St. Louis, MO). Samples were 10 μM of tripeptide in 70/30 water/methanol containing 0.1% acetic acid. They were electrosprayed at a flow rate of 3 μL/min with air being the nebulizer gas. Ions thus formed were sampled from the atmospheric pressure ion source into an "enclosed" quadrupolar lens region (q0), where multiple collisions with the "curtain-gas" molecules of nitrogen sampled with the ions occurred. When needed, first-generation product ions, b_2 and a_2, were first produced in the region between the orifice and q0, and collisionally deactivated downstream. Thermalization of the sampled ions in the lens region was highly efficient;[58−65] threshold energies determined with our apparatus using lens collision energies that were higher by 4−6 eV (laboratory frame) than those used in the actual determination (8−12 eV) were indistinguishable from those acquired under standard conditions. CID was performed with argon as the neutral gas. (Xenon was also used initially and its performance was compared with that of argon.[39,56,57] The modeled threshold curves at 0 K determined with Xe had larger slopes than those determined with Ar, and the threshold energies were typically smaller by <0.1 eV; however, the plots were more scattered. This, in combination with xenon's higher cost, resulted in our choice of argon.) The gas pressure in q2 was continuously monitored with an upstream baritron gauge, the readout of which was converted into collision-gas thickness (CGT, the product of the neutral gas number density and the length of q2)[66] by the mass spectrometric software.

The threshold energy, E_0, for the CID of a given ion was determined by using the curve-fitting and modeling program, CRUNCH, developed by Armentrout and co-workers.[67−73] Modeling took into account the large number of degrees of freedom in the fragmenting ions and the additional internal energy (the "kinetic shift") required to increase the fragmentation rate to a magnitude that was measurable in our apparatus. Determination of E_0 required the vibrational frequencies and rotational constants of the precursor ions and the transition states. These were obtained from the DFT calculations and are listed in Table 4S in the Supporting Information. As before,[39,56,57] the dissociation cross-sections, $\sigma(E)$, of the product ions were determined as a function of the center-of-mass energies at four argon pressures, typically at CGT values of 100×10^{12}, 75×10^{12}, 50×10^{12}, and 25×10^{12} atoms cm^{-2}. To eliminate the effects of multiple collisions, the E_0 value was obtained from a threshold curve constructed only from $\sigma(E)$ at zero CGT, by extrapolation via least-squares fits of presumed exponential functions.[39,56,57] A typical threshold curve in the present work comprises 90 $\sigma(E)$ values over an E_{cm} range of 0−6 eV. The E_0 value for each fragmentation reaction examined was determined in duplicate. As in previous investigations,[39,56,57] ion energy distributions in the laboratory frame are ap proximately 2 eV (full width at half maximum). Evaluation of

TABLE 2: Threshold Energies and $\Delta H^{\ddagger}_0$ Values for GAG-Derived Ions

reaction	E_0, eV	E_0(k.s.), eV	$\Delta H^{\ddagger}_0$(exptl), kcal/mol	ΔH°_0(theory), kcal/mol
$b_2 \rightarrow a_2$	1.74	1.30(+0.08/−0.09)	30.0(+1.8/−2.1)	29.9
$b_2 \rightarrow a_1$	2.41	1.72(+0.09/−0.13)	39.8(+2.1/−3.0)	43.2
		1.59(+0.08/−0.12)[a]	36.7(+1.8/−2.8)[a]	
$a_2 \rightarrow a_1$	1.75	1.49(+0.08/−0.10)	34.3(+1.8/−2.3)	34.0
		1.45(+0.08/−0.10)[b]	33.5(+1.8/−2.3)[b]	
$a_2 \rightarrow$ internal iminium	1.67	1.41(+0.09/−0.12)	32.4(+2.1/−2.8)	34.0

[a] In competition with $b_2 \rightarrow a_2$. [b] In competition with $a_2 \rightarrow$ internal iminium.

TABLE 3: Threshold Energies and $\Delta H^{\ddagger}_0$ Values for AGG-Derived Ions

reaction	E_0, eV	E_0(k.s.), eV	$\Delta H^{\ddagger}_0$(exptl), kcal/mol	ΔH°_0(theory), kcal/mol
$b_2 \rightarrow a_2$	1.89	1.46(+0.08/−0.10)	33.7(+1.8/−2.3)	33.7
$b_2 \rightarrow a_1$	1.93	1.42(+0.08/−0.10)	32.7(+1.8/−2.3)	31.4
		1.37(+0.08/−0.09)[a]	31.6(+1.8/−2.1)[a]	
$a_2 \rightarrow a_1$	1.70	1.51(+0.10/−0.12)	34.8(+2.3/−2.8)	34.9

[a] In competition with $b_2 \rightarrow a_2$.

E_0 took into account the ion energy distribution[74] and the thermal motion of argon.[74,75] We assume the ion and the argon temperatures to be 298 K. Possible errors due to uncertainty of the ion and argon temperatures were estimated in the same manner as previously reported.[39] Because we assume that the ion temperature fell within 298 ± 100 K and the argon temperature was ≤298 K, with 198 K being the lower limit, the positive and negative uncertainties are different and were propagated separately.[39] Tables 2 and 3 list the E_0 values for respectively GGA and AGA before and after kinetic shift consideration (E_0 and E_0(k.s.), respectively) with the uncertainties in parentheses.

Threshold CID is most commonly applied to measuring binding enthalpies of metal ions (M^+) to ligands (L). The E_0 of the reaction $M^+{-}L \rightarrow M^+ + L$ gives the enthalpy change of the reaction at 0 K, ΔH°_0, the binding energy. An inherent assumption in equating E_0 to ΔH°_0 is that the dissociation is barrierless, usually valid for the dissociation of most metal−ligand complexes where L contains only one metal-binding site. By contrast, rearrangement reactions, including the dissociation reactions that are examined in this study, have significant barriers for dissociation. For these reactions, the E_0 values are measures of the barrier heights of the rate-determining steps in terms of enthalpies at 0 K or $\Delta H^{\ddagger}_0$. Tables 2 and 3 also list the $\Delta H^{\ddagger}_0$ values with the uncertainties in parentheses. Calculated ΔH°_0 values are also listed for comparison.

Results and Discussion

In general, the fragmentation reactions of GAG, AGG, and GGG[39] show a lot of similarities. All protonated tripeptides fragment to give abundant b_2, a_2, and a_1 ions;[39] in addition, protonated GAG fragments prominently to give a product ion at 44 Th, an iminium ion originating from the central, alanyl residue. All residues in GGG are identical; thus any internal iminium ion produced is indistinguishable from the a_1 ion.[39] Differentiation between the two is possible in AGG; however, no internal iminium ion (due to the glycyl residue) is observable. This difference between protonated GAG and AGG is emphasized and clearer in a comparison of the fragmentation of their respective a_2 ions (see later).

Fragmentation of the b_2 to the a_2 Ion. In the earlier study on protonated GGG,[39] it was reported that the b_2 ion, a protonated oxazolone,[24,25,27,37] fragments to the a_2 ion via a number of steps. Collisional activation leads to opening of the oxazolone ring to give a complex comprising the iminium form of the a_2 ion and CO. This intermediate then dissociates to give the iminium ion of a_2 (and CO). These steps are similar to those proposed previously by Harrison and co-workers[24,25] and by Paizs et al.[41] The iminium form (see structure **3** for the analogous structure of GAG), however, is not the lowest energy isomer of the a_2 ion; the cyclic form, a protonated 4-imidazolidone (see structure **4** for the analogous structure of GAG), is lower by 8.9 kcal/mol in free energy at 298 K. Furthermore, the free-energy barrier of this isomerization step is only 11.9 kcal/mol.

Figure 1a shows the reaction profile for the dissociation of the b_2 to the a_2 ion from GAG. Energies are in kcal/mol: ΔG°_{298} values are shown in regular font while ΔH°_0 values are parenthesized in italics. Details of the profile are qualitatively identical with those in GGG, but differ quantitatively. In general, all energies (relative to the b_2 ion) are lower on the GAG surface than on the GGG surface. Table 1 compares the ΔG°_{298} and ΔH°_0 values of the minima and transition-state structures. The inductive effect of the methyl side chain in the alanyl residue confers considerable charge stabilization on the proximal $H{-}N^+$ group and results in a rather dramatic lowering of the energies. This is especially evident in the iminium form of the a_2 ion, structure **3**, in GAG. This stabilization renders the iminium form (plus CO) only 2.3 kcal/mol higher in free energy than the b_2 ion, whereas in GGG structure **3** + CO is 13.1 kcal/mol higher (in free energy). The cyclic form of the a_2 ion, structure **4**, is lower in free energy than the open form, structure **3**, by only 0.7 kcal/mol in GAG versus 8.9 kcal/mol in GGG. This particularly effective stabilization of structure **3** by the methyl side chain is probably due to hyperconjugation with the charged center via the unsaturated C═N bond.

By contrast, the relative energies of the minima and transition state structures on the AGG surface (Figure 1b) are comparable to those on the GGG surface with one notable exception, structure **4** + CO (this and the primes in subsequent structures are dropped in comparisons among the three tripeptides), which has the lowest free energy and enthalpy of all three 4-imidazolidones. For structures **2** and **3**, and transition states **TS(1→2)** and **TS(3→4)**, the similarity between AGG and GGG is in accordance with the expectation that the methyl side chain of the N-terminal alanyl residue should exert little effect on the $H{-}N^+$ group in the second residue. Cyclization in forming structure **4**, amine-protonated 4-imidazolidone, transfers the formal charge center from the nitrogen of the second residue to the nitrogen of the first residue. This puts the formal charge center in the vicinity of the methyl group. For AGG, structure **4** is protonated 5-methyl-4-imidazolidone, whereas for GAG, it is protonated 2-methyl-4-imidazolidone. At the B3LYP/6-31++G(d,p) level of theory, the former is lower than the latter by 0.7 kcal/mol in free energy; protonated 2-methyl-4-imidazolidone is lower than protonated 4-imidazolidone (from GGG) by 2.6 kcal/mol in relative free energy (to the b_2 ion).

As detailed earlier,[39] the threshold CID experiment measures

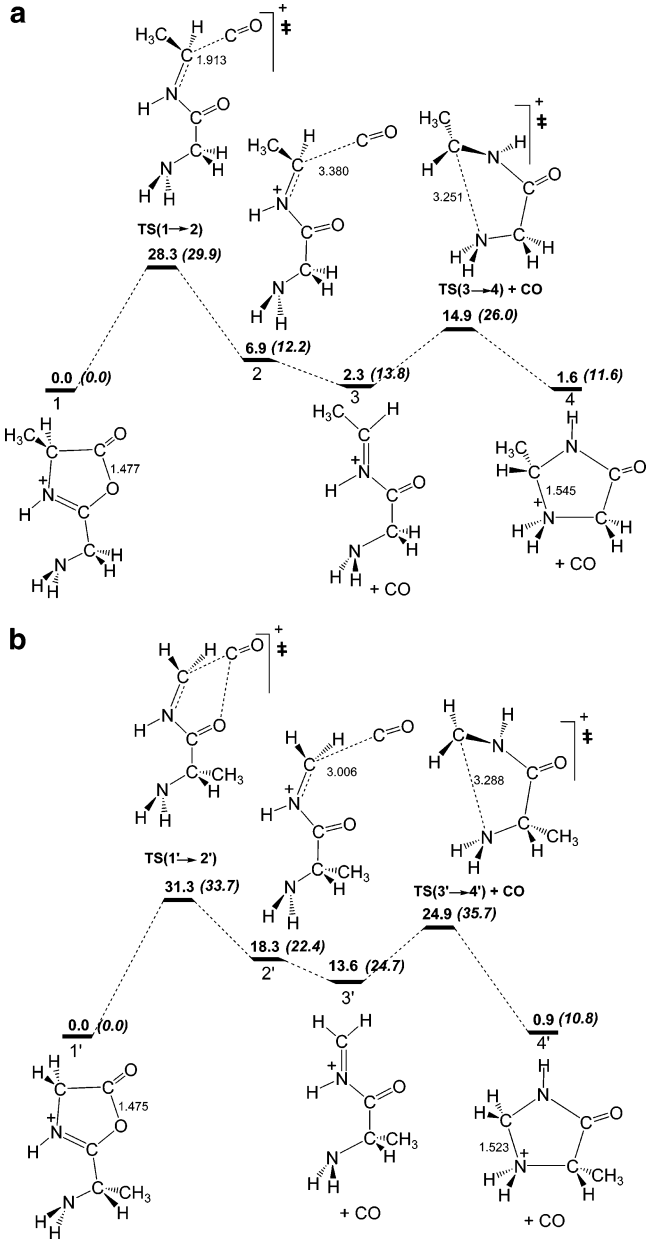

Figure 1. Energy profiles for the fragmentation of b_2 to a_2 ion: (a) GAG and (b) AGG. $\Delta G°_{298}$ values (in kcal/mol) are shown in regular font and $\Delta H°_0$ values are parenthesized in italics.

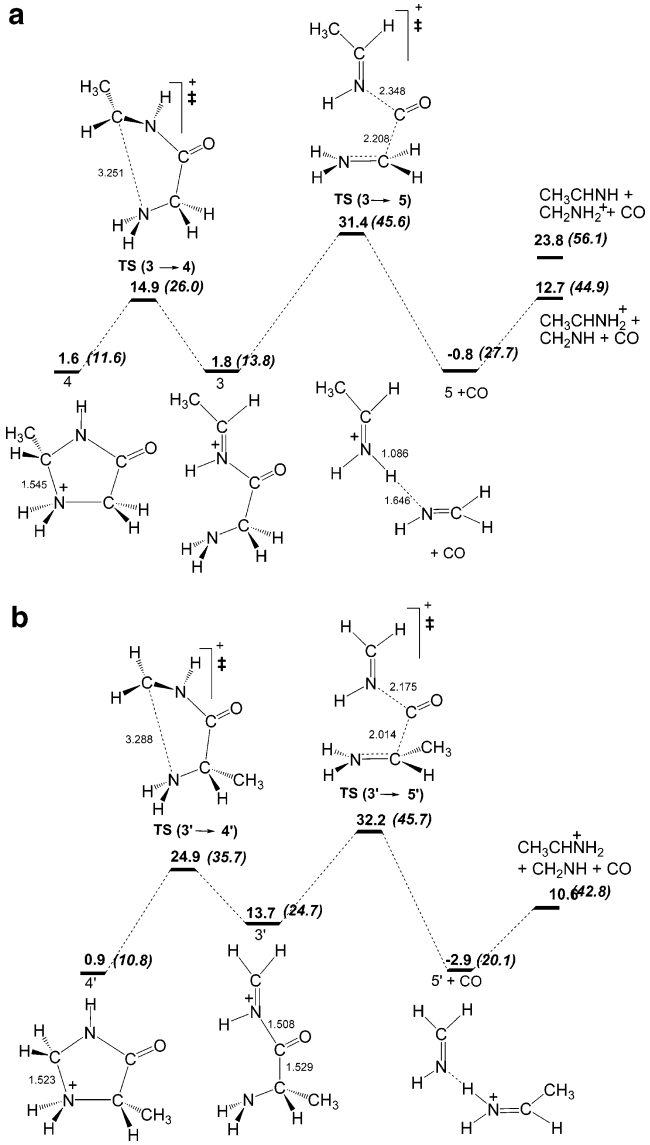

Figure 2. Energy profiles for the fragmentation of a_2 to a_1 ion: (a) GAG and (b) AGG. $\Delta G°_{298}$ values (in kcal/mol) are shown in regular font and $\Delta H°_0$ values are parenthesized in italics.

the fragmentation barrier in terms of enthalpy at 0 K. The rate-determining step in the fragmentation of the b_2 to the a_2 ion is the ring-opening step of the oxazolone. For GAG, the experimental barrier, $\Delta H^{\ddagger}_0$(exptl), is 30.0(+1.8/−2.1) kcal/mol, in good agreement with the calculated barrier height of **TS(1→2)** in terms of enthalpy at 0 K, $\Delta H^{\ddagger}_0$(theory), at 29.9 kcal/mol (Table 2). For AGG, $\Delta H^{\ddagger}_0$(exptl) is 33.7(+1.8/−2.3) kcal/mol, again in good agreement with $\Delta H^{\ddagger}_0$ (theory) at 33.7 kcal/mol (Table 3). As discussed earlier,[39] DFT calculations at the B3LYP/6-31++G(d,p) level of theory have been found to deviate by no more than 2−3 kcal/mol from the best experimental values.[36−38,54,55] The agreement between the experimental and calculated $\Delta H^{\ddagger}_0$ values for GAG and AGG lends credence to the fragmentation mechanism depicted in Figure 1 and supports the earlier findings based on GGG.[39]

Fragmentation of the a_2 to the a_1 Ion. Figure 2a shows the reaction profile for the dissociation of the a_2 to the a_1 ion from GAG, while Figure 2b shows that from AGG. Both profiles share many similarities with the analogous profile in GGG. Collisional activation of the a_2 ion, structure **4**, leads first to ring opening and formation of the iminium form of the a_2 ion, structure **3**. The C−C and the C−N bonds that bracket the carbonyl group then lengthen to form the critical transition state **TS(3→5)**. The components then rearrange to form structure **5**, an iminium−imine complex bridged by a proton, and CO. In both GAG and AGG, structure **5** is a protonated ethanimine solvated by a methanimine. In GAG, the ethanimine originates from the *second*, alanyl residue, whereas in AGG, the ethanimine originates from the *first*, alanyl residue. Thus in GAG there is *proton transfer* between the imine of the first, glycyl residue and the "internal" imine of the second, alanyl residue. The proton affinities of methanimine and ethanimine are 203.8 and 211.5 kcal/mol, respectively;[76] thus proton transfer from the protonated methanimine to the ethanimine component is expected to occur efficiently. Subsequent dissociation of the proton-bound complex gives the products protonated ethanimine and methanimine. The former is the internal iminium ion in GAG. By contrast, dissociation of the a_2 ion from AGG lacks

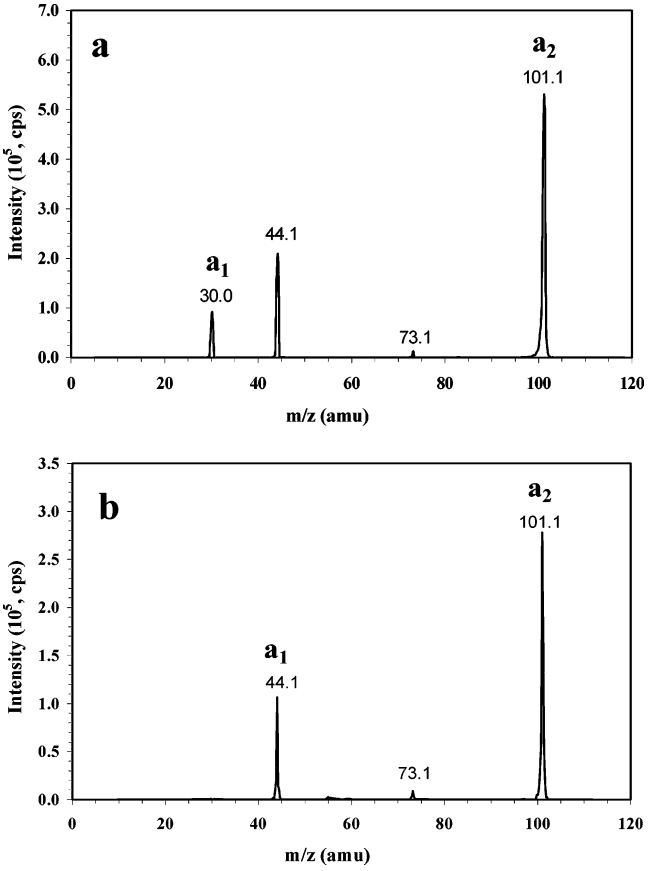

Figure 3. CID mass spectra of the a_2 ion in (a) GAG and (b) AGG at center-of-mass collision energies of 3.0 eV.

this proton-transfer step as the first residue constitutes the protonated ethanimine component in the proton-bridged complex.

Figure 3 shows the CID mass spectra of the a_2 ion from (a) GAG and (b) AGG at a center-of-mass collision energy (E_{cm}) of 3.0 eV. It is evident that in GAG, fragmentation of the a_2 ion results in both the a_1 ion (protonated methanimine) at 30 Th and the internal iminium ion (protonated ethanimine) at 44 Th, whereas in AGG, fragmentation results in only the a_1 ion (protonated ethanimine) at 44 Th. The proton-bridged imine complex, **5**, at 73 Th is also evident. The ratio of the a_1 to the internal iminium ion in GAG increases from approximately 0.2 at an $E_{cm} = 1.5$ eV, to 0.5 at an $E_{cm} = 2.5$ eV, to 0.6 at an $E_{cm} = 3.5$ eV, and to 0.7 at an $E_{cm} = 4.5$ eV. At low collision energy, the rearrangement reaction gives predominately protonated ethanimine, whereas at high collision energy, dissociation proceeds via vibrationally excited **TS(3→5)** and structure **5**, which produces more of the energetically unfavorable a_1 ion (Figure 2a). Formation of the a_1 ion here requires dissociation before internal proton transfer from the protonated methanimine to ethanimine can occur. In AGG, no internal proton transfer occurs; thus dissociation gives only the a_1 ion, protonated ethanimine, irrespective of the energy content of the dissociating complex (Figure 2b). Support for the above mechanism in the fragmentation of the a_2 ion was provided by Harrison et al.,[77] who examined the dissociation of the a_2 ions of glycylalaninamide and alanylglycinamide, and extended the results reported here to amides of more complex dipeptides. When the imine of the first residue had a lower PA than that of the second residue, in general both protonated imines were observable upon CID of the a_2 ion. However, when the former had a higher PA than the latter, only the protonated imine of the first residue, the a_1 ion, was present. These results are in accordance with the mechanism discussed above.

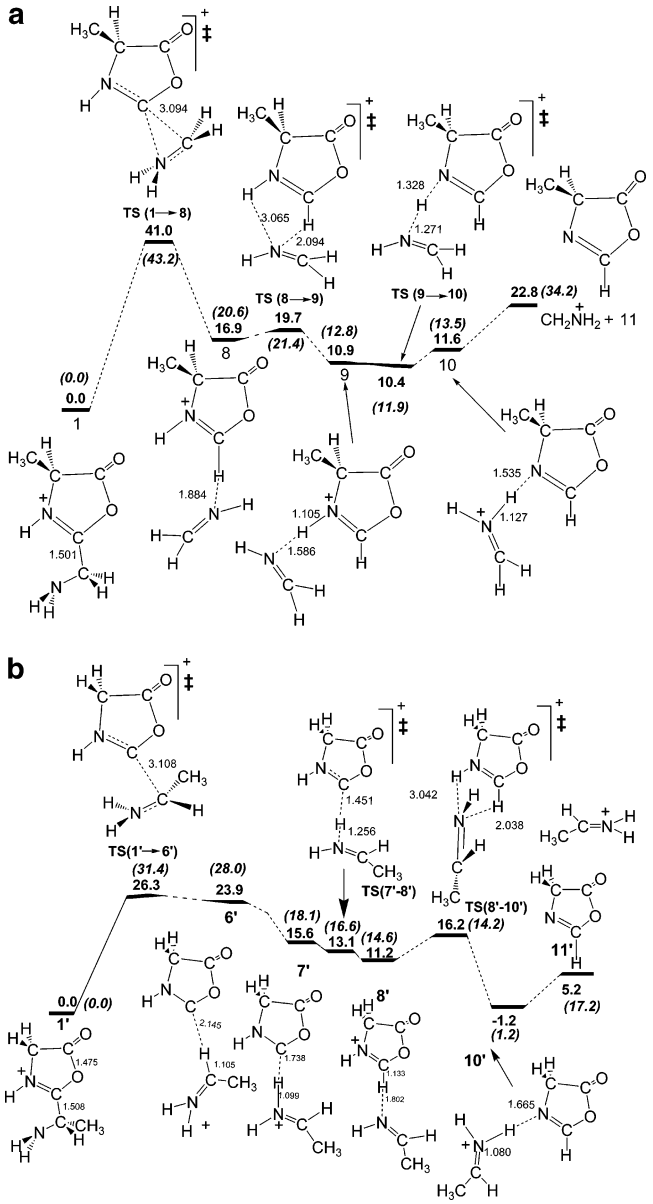

Figure 4. Energy profiles for the fragmentation of b_2 to a_1 ion: (a) GAG and (b) AGG. $\Delta G°_{298}$ values (in kcal/mol) are shown in regular font and $\Delta H°_0$ values are parenthesized in italics.

For GAG, the $\Delta H^{\ddagger}_0$(exptl) values for the a_2 to a_1 and the a_2 to the internal iminium fragmentations are 34.3(+1.8/−2.3) and 32.4(+2.1/−2.8) kcal/mol, respectively. When the two are considered in competition, the a_2 to the a_1 dissociation becomes 33.5(+1.8/−2.3) kcal/mol. All these threshold CID values are in good agreement with the $\Delta H^{\ddagger}_0$(theory) value of 34.0 kcal/mol (Table 2). For AGG, the $\Delta H^{\ddagger}_0$(exptl) for the a_2 to the a_1 dissociation is 34.8(+2.3/−2.8) kcal/mol, in good agreement with the $\Delta H^{\ddagger}_0$(theory) of 34.9 kcal/mol (Table 3).

Fragmentation of the b_2 to the a_1 Ion. Figure 4 shows the reaction profile for the dissociation of the b_2 to the a_1 ion from (a) GAG and (b) AGG. In contrast to the fragmentations discussed earlier, there is considerable difference between the fragmentation of GAG and AGG ions. The reaction profile of GAG resembles quite closely that of GGG.[39] This is evident in Table 1. Charge stabilization by the methyl side chain in the second, alanyl residue plays a minor role in the minima and transition state structures in the GAG profile. The critical

transition state, **TS(1→8)**, is best described as a complex between the a_1 ion and a carbene. The transient carbene postulated here is stabilized by π-donation from adjacent nitrogen and oxygen atoms. Singlet carbenes stabilized by two adjacent nitrogen π-donors are sufficiently stable to crystallize.[78,79] The fact that this transition state is slightly higher in energy (41.0 versus 39.3 kcal/mol in terms of free energy) in GAG than in GGG probably reflects a *better charge stabilization in the b_2 ion* of GAG than GGG. The corresponding transition state in AGG, **TS(1′→6′)**, is much lower in energy because of the inductive effect of the methyl group in the a_1 ion component, $CH_3CH{=}NH_2^+$. Ion **8** differs from **6** in that the former is a protonated oxazolone solvated by an imine, while the latter is an iminium ion solvated by a carbene. These two ions then give different transition states and minima, which eventually lead to structure **10**, a complex between the a_1 ion and an oxazolone, which is again shared between the two profiles. Despite differences in details of the intervening structures and transition states, the two profiles share the common elements of a proton transfer from the terminal amino group to the carbene carbon and a second proton transfer from the ring nitrogen back to the terminal amino group to give the common structure **10**.

The experimental $\Delta H^{\ddagger}_0$ values of 39.8(+2.1/−3.0) kcal/mol for GAG and 32.7(+1.8/−2.3) kcal/mol for AGG are in accord with the $\Delta H^{\ddagger}_0$ values of 43.2 kcal/mol for GAG and 31.4 kcal/mol for AGG calculated by DFT. Tables 2 and 3 also list the $\Delta H^{\ddagger}_0$(exptl) values when the b_2 to a_1 fragmentation is considered in competition with the b_2 to a_2 fragmentation. For AGG, there is only 1.1 kcal/mol difference between the two $\Delta H^{\ddagger}_0$(exptl) values; thus both values are in good agreement with the ΔH°_0(theory) of 31.4 kcal/mol. For GAG, the difference between the $\Delta H^{\ddagger}_0$(exptl) values is larger at 3.1 kcal/mol. The calculated ΔH°_0 lies just outside of the experimental uncertainties of $\Delta H^{\ddagger}_0$ when the b_2 to a_1 fragmentation is considered independently. In comparison with the other fragmentation reactions, fragmentation of the b_2 to the a_1 ion involves the largest kinetic shift of 0.69 eV, which may have introduced an error larger than the ±0.1 eV used in calculating the overall uncertainties.[39] The calculated ΔH°_0 appears to be in better agreement with the experimental $\Delta H^{\ddagger}_0$ when the b_2 to the a_1 fragmentation is considered independently rather than in competition with the b_2 to the a_2 fragmentation. This is also true in GGG.[39] However, there are too few (two) data points to draw a conclusion.

Conclusions

Findings in this study with GAG and AGG confirm and extend those in an earlier study on GGG.[39] The presence of the methyl group in the alanyl residue *proximal* to the charge center stabilizes the structure and results in comparatively lower energy than the corresponding structure in GGG. Fragmentation of the b_2 to a_2 ion from GAG and AGG is qualitatively similar to that from GGG; stabilization by the methyl group results in generally lower energies for GAG. Fragmentation of the a_2 ion from GAG produces both the a_1 (protonated methanimine) and the internal iminium ion (protonated ethanimine). By contrast, fragmentation of the a_2 ion from AGG produces only the a_1 ion (protonated ethanimine). In GAG, formation of the internal iminium ion requires an intramolecular proton transfer in the proton-bridged complex after cleavage of CO, which is absent in AGG. The critical transition state in the fragmentation of the b_2 to a_1 ion is best described as a complex between the a_1 ion and a carbene. Although details differ, in both GAG and AGG, there is a proton transfer from the terminal amino group to the carbene carbon and a second proton transfer from the ring nitrogen back to the terminal amino group. Separation of the components then yields the a_1 ion and a neutral oxazolone.

Acknowledgment. We thank Professor P. B. Armentrout for making his CRUNCH program available to us and Professor A. G. Harrison for helpful discussion. This work was supported by the Natural Sciences and Engineering Research Council (NSERC) of Canada, MDS Sciex, the Canadian Foundation of Innovation (CFI), the Ontario Innovation Trust (OIT), and York University.

Supporting Information Available: Listings of total electronic energies (E_t), enthalpies at 0 K (H°_0), free energies at 298 K (G°_{298}), relative enthalpies (ΔH°_0), and relative free energies (ΔG°_{298}) for GAG- and AGG-derived ions (Table 1S); Cartesian coordinates of GAG-derived structures (Table 2S); Cartesian coordinates of AGG-derived structures (Table 3S); and vibrational frequencies and rotational constants of the precursor ions and transition states (Table 4S). This material is available free of charge via the Internet at http://pubs.acs.org.

References and Notes

(1) Aebersold, R.; Mann, M. *Nature* **2003**, *422*, 198−207.
(2) Pappayanopolous, I. *Mass Spectrom. Rev.* **1995**, *14*, 49−73.
(3) O'Hair, R. A. J. *J. Mass Spectrom.* **2000**, *35*, 1377−1381.
(4) Schlosser, A.; Wolf, D. L. *J. Mass Sepctrom.* **2000**, *35*, 1382−1390.
(5) Polce, M. J.; Ren, D.; Wesdemiotis, C. *J. Mass Spectrom.* **2000**, *35*, 1391−1398.
(6) Wysocki, V. H.; Tsaprailis, G.; Smith, L. L.; Breci, L. A. *J. Mass Spectrom.* **2000**, *35*, 1399−1406.
(7) Tabb, D. L.; Smith, L. L.; Breci, L. A.; Wysocki, V. H.; Lin, D.; Yates, J. R., III *Anal. Chem.* **2003**, *75*, 1155−1163.
(8) Breci, L. A.; Tabb, D. L.; Yates, J. R., III; Wysocki, V. H. *Anal. Chem.* **2003**, *75*, 1963−1971.
(9) Tabb, D. L.; Huang, Y.; Wysocki, V. H.; Yates, J. R., III *Anal. Chem.* **2004**, *76*, 1243−1248.
(10) Huang, Y.; Triscari, J. M.; Pasa-Tolic, L.; Anderson, G. A.; Lipton, M. S.; Smith, R. D.; Wysocki, V. H. *J. Am. Chem. Soc.* **2004**, *126*, 3034−3035.
(11) Kapp, E. A.; Schütz, F.; Reid, G. E.; Eddes, J. S.; Moritz, R. L.; O'Hair, R. A. J.; Speed, T. P.; Simpson, R. J. *Anal. Chem.* **2003**, *75*, 6251−6264.
(12) Eng, J. K.; McCormack, A. L.; Yates, J. R., III *J. Am. Soc. Mass Spectrom.* **1994**, *5*, 976−989.
(13) Perkins, D. N.; Pappin, D. J.; Creasy, D. M.; Cottrell, J. S. *Electrophoresis* **1999**, *20*, 3551−3567.
(14) Clauser, K. R.; Baker, P. R.; Burlingame, A. L. *Anal. Chem.* **1999**, *71*, 2871−2882.
(15) McCormack, A. L.; Jones, J. L.; Wysocki, V. H. *J. Am. Soc. Mass Spectrom.* **1992**, *3*, 859−862.
(16) Jones, J. L.; Dongre, A. R.; Somogyi, A.; Wysocki, V. H. *J. Am. Chem. Soc.* **1994**, *116*, 8368−8369.
(17) Dongre, A. R.; Jones, J. L.; Somogyi, A.; Wysocki, V. H. *J. Am. Chem. Soc.* **1996**, *118*, 8365−8374.
(18) Dongre, A. R.; Somogyi, A.; Wysocki, V. H. *J. Mass Spectrom.* **1996**, *31*, 339−350.
(19) Tsaprailis, G.; Nair, H.; Somogyi, A.; Wysocki, V. H.; Zhong, W.; Futrell, J. H.; Summerfield, S. G.; Gaskell, S. J. *J. Am. Chem. Soc.* **1999**, *121*, 5142−5154.
(20) Tsaprailis, G.; Somogyi, A.; Nikolaev, E. N.; Wysocki, V. H. *Int. J. Mass Spectrom.* **2000**, *195/196*, 467−479.
(21) Burlet, O.; Yang, C.-Y.; Gaskell, S. J. *J. Am. Soc. Mass Spectrom.* **1992**, *3*, 337−344.
(22) Cox, K. A.; Gaskell, S. J.; Morris, M.; Whiting, A. *J. Am. Soc. Mass Spectrom.* **1996**, *7*, 522−531.
(23) Summerfield, S. G.; Whiting, A.; Gaskell, S. J. *Int. J. Mass Spectrom.* **1997**, *162*, 149−161.
(24) Yalcin, T.; Khouw, C.; Csizmadia, I. G.; Peterson, M. R.; Harrison, A. G. *J. Am. Soc. Mass Spectrom.* **1995**, *6*, 1164−1174.
(25) Yalcin, T.; Csizmadia, I. G.; Peterson, M. R.; Harrison, A. G. *J. Am. Soc. Mass Spectrom.* **1996**, *7*, 233−242.
(26) Ambihapathy, K.; Yalcin, T.; Leung, H.-W.; Harrison, A. G. *J. Mass Spectrom.* **1997**, *32*, 209−215.
(27) Nold, M. J.; Wesdemiotis, C.; Yalcin, T.; Harrison, A. G. *Int. J. Mass Spectrom. Ion Processes* **1997**, *164*, 137−153.

(28) Harrison, A. G.; Csizmadia, I. G.; Tang, T.-H. *J. Am. Soc. Mass Spectrom.* **2000**, *11*, 427−436.
(29) Reid, G. E.; Simpson, R. J.; O'Hair, R. A. J. *Int. J. Mass Spectrom.* **1999**, *190*/*191*, 209−230.
(30) Paizs, B.; Lendvay, G.; Vékey, K.; Suhai, S. *Rapid Commun. Mass Spectrom.* **1999**, *13*, 525−533.
(31) Csonka, I. P.; Paizs, B.; Lendvay, G.; Suhai, S. *Rapid Commun. Mass Spectrom.* **2000**, *14*, 417−431.
(32) Paizs, B.; Suhai, S. *Rapid Commun. Mass Spectrom.* **2001**, *15*, 651−663.
(33) Paizs, B.; Suhai, S. *Rapid Commun. Mass Spectrom.* **2001**, *15*, 2307−2323.
(34) Paizs, B.; Suhai, S. *Rapid Commun. Mass Spectrom.* **2002**, *16*, 375−389.
(35) Paizs, B.; Suhai, S. *J. Am. Soc. Mass Spectrom.* **2004**, *15*, 103−113.
(36) Rodriquez, C. F.; Cunje, A.; Shoeib, T.; Chu, I. K.; Hopkinson, A. C.; Siu, K. W. M. *J. Phys. Chem. A* **2000**, *104*, 5023−5028.
(37) Rodriquez, C. F.; Shoeib, T.; Chu, I. K.; Siu, K. W. M.; Hopkinson, A. C. *J. Phys. Chem. A* **2000**, *104*, 5335−5342.
(38) Rodriquez, C. F.; Cunje, A.; Shoeib, T.; Chu, I. K.; Hopkinson, A. C.; Siu, K. W. M. *J. Am. Chem. Soc.* **2001**, *123*, 3006−3012.
(39) El Aribi, H.; Rodriquez, C. F.; Almeida, D. R. P.; Ling, Y.; Mak, W. W.-N.; Hopkinson, A. C.; Siu, K. W. M. *J. Am. Chem. Soc.* **2003**, *125*, 9229−9236.
(40) Grewal, R. N.; El Aribi, H.; Harrison, A. G.; Siu, K. W. M.; Hopkinson, A. C. *J. Phys. Chem. B* **2004**, *108*, 4899−4908.
(41) Paizs, B.; Szlávik, Z.; Lendvay, G.; Vékey, K.; Suhai, S. *Rapid Commun. Mass Spectrom.* **2000**, *14*, 746−755.
(42) Frisch, M. J.; Trucks, G. W.; Schlegel, H. B.; Scuseria, G. E.; Robb, M. A.; Cheeseman, J. R.; Zakrzewski, V. G.; Montgomery, J. A.; Stratmann, R. E.; Burant, J. C.; Dapprich, S.; Millam, J. M.; Daniels, A. D.; Kudin, K. N.; Strain, M. C.; Farkas, O.; Tomasi, J.; Barone, V.; Cossi, M.; Cammi, R.; Mennucci, B.; Pomelli, C.; Adamo, C.; Clifford, S.; Ochterski, J.; Petersson, G. A.; Ayala, P. Y.; Cui, Q.; Morokuma, K.; Salvador, P.; Dannenberg, J. J.; Malick, D. K.; Rabuck, A. D.; Raghavachari, K.; Foresman, J. B.; Cioslowski, J.; Ortiz, J. V.; Baboul, A. G.; Stefanov, B. B.; Liu, G.; Liashenko, A.; Piskorz, P.; Komaromi, I.; Gomperts, R.; Martin, R. L.; Fox, D. J.; Keith, T.; Al-Laham, M. A.; Peng, C. Y.; Nanayakkara, A.; Challacombe, M.; Gill, P. M. W.; Johnson, B. G.; Chen, W.; Wong, M. W.; Andres, J. L.; Gonzalez, C.; Head-Gordon, M.; Replogle, E. S.; Pople, J. A. *Gaussian 98*, rev. A.11; Gaussian, Inc.: Pittsburgh, PA, 2001.
(43) Becke, A. D. *Phys. Rev.* **1988**, *A38*, 3098−3100.
(44) Becke, A. D. *J. Chem. Phys.* **1993**, *98*, 5648−5652.
(45) Lee, C.; Yang, W.; Parr, R. G. *Phys. Rev.* **1988**, *B37*, 785−789.
(46) Ditchfield, R.; Hehre, W. J.; Pople, J. A. *J. Chem. Phys.* **1971**, *54*, 724−728.
(47) Hehre, W. J.; Ditchfield, R.; Pople, J. A. *J. Chem. Phys.* **1972**, *56*, 2257−2261.
(48) Hariharan, P. C.; Pople, J. A. *Mol. Phys.* **1974**, *27*, 209−214.
(49) Gordon, M. S. *Chem. Phys. Lett.* **1980**, *76*, 163−168.
(50) Hariharan, P. C.; Pople, J. A. *Theor. Chim. Acta* **1973**, *28*, 213−222.
(51) Clark, T.; Chandrasekhar, J.; Spitznagel, G. W.; Schleyer, P. v. R. *J. Comput. Chem.* **1983**, *4*, 294−301.
(52) Gonzalez, C.; Schlegel, H. B. *J. Chem. Phys.* **1989**, *90*, 2154−2161.
(53) Gonzalez, C.; Schlegel, H. B. *J. Phys. Chem.* **1990**, *94*, 5523−5527.
(54) Shoeib, T.; Rodriquez, C. F.; Siu, K. W. M.; Hopkinson, A. C. *Phys. Chem. Chem. Phys.* **2001**, *3*, 853−861.
(55) Addario, V.; Guo, Y.; Chu, I. K.; Ling, Y.; Ruggerio, G.; Rodriquez, C. F.; Hopkinson, A. C.; Siu, K. W. M. *Int. J. Mass Spectrom.* **2002**, *219*, 101−114.
(56) El Aribi, H.; Shoeib, T.; Ling, Y.; Rodriquez, C. F.; Hopkinson, A. C.; Siu, K. W. M. *J. Phys. Chem. A* **2002**, *106*, 2908−2914.
(57) El Aribi, H.; Rodriquez, C. F.; Shoeib, T.; Ling, Y.; Hopkinson, A. C.; Siu, K. W. M. *J. Phys. Chem. A* **2002**, *106*, 8798−8805.
(58) Douglas, D. J. *J. Phys. Chem.* **1982**, *86*, 185−191.
(59) Douglas, D. J.; French, J. B. *J. Am. Soc. Mass Spectrom.* **1992**, *3*, 398−408.
(60) Covey, T.; Douglas, D. J. *J. Am. Soc. Mass Spectrom.* **1993**, *4*, 616−623.
(61) Goeringer. D. E.; Asano, K. G.; McLuckey, S. A. *Int. J. Mass Spectrom.* **1999**, *182*/*183*, 275−288.
(62) Asano, K. G.; Goeringer, D. E.; McLuckey, S. A. *Int. J. Mass Spectrom.* **1999**, *185*/*186*/*187*, 207−219.
(63) Drahos, L.; Heeren, R. M. A.; Collette, C.; De Pauw, E.; Vékey, K. *J. Mass Spectrom.* **1999**, *34*, 1373−1379.
(64) Schneider, B. B.; Chen, D. D. Y. *Anal. Chem.* **2000**, *72*, 791−799.
(65) Schneider, B. B.; Douglas, D. J.; Chen, D. D. Y. *J. Am. Soc. Mass Spectrom.* **2001**, *12*, 772−779.
(66) Dawson, P. H.; French, J. B.; Buckley, J. A.; Douglas, D. J.; Simmons, D. *Org. Mass Spectrom.* **1982**, *17*, 205−211.
(67) Ervin, K. M.; Armentrout, P. B. *J. Chem. Phys.* **1985**, *83*, 166−189.
(68) Weber, M. E.; Elkind, J. L.; Armentrout, P. B. *J. Chem. Phys.* **1986**, *84*, 1521−1529.
(69) Schultz, R. H.; Crellin, K. C.; Armentrout, P. B. *J. Am. Chem. Soc.* **1991**, *113*, 8590−8601.
(70) Dalleska, N. F.; Honma, K.; Sunderlin, L. S.; Armentrout, P. B. *J. Am. Chem. Soc.* **1994**, *116*, 3519−3528.
(71) Shvartsburg, A. A.; Ervin, K. M.; Frederick, J. H. *J. Chem. Phys.* **1996**, *104*, 8458−8469.
(72) Rodgers, M. T.; Ervin, K. M.; Armentrout, P. B. *J. Chem. Phys.* **1997**, *106*, 4499−4508.
(73) Rodgers, M. T.; Armentrout, P. B. *J. Chem. Phys.* **1998**, *109*, 1787−1800.
(74) Lifshitz, C.; Wu, R. L. C.; Tiernan, T. O.; Terwilliger, D. T. *J. Chem. Phys.* **1978**, *68*, 247−260.
(75) Chantry, P. J. *J. Chem. Phys.* **1971**, *55*, 2746−2759.
(76) NIST Webbook: http://webbook.nist/gov.
(77) Harrison, A. G.; Young, A. B.; Schnoelzer, M.; Paizs, B. *Rapid Commun. Mass Spectrom.* **2004**, *18*, 1635−1640.
(78) Arduengo, A. J., III; Harlow, R. L.; Kline, M. *J. Am. Chem. Soc.* **1991**, *113*, 361−363.
(79) Magill, A. M.; Cavell, K. J.; Yates, B. F. *J. Am. Chem. Soc.* **2004**, *126*, 8717−8724.